A Trisubstituted 1,4-Diazepine-3-one-Based Dipeptidomimetic: Conformational Characterization by NMR and Computer Simulation

Maria Pellegrini,[†] **Iris S. Weitz,**[‡] **Michael Chorev,**[‡,§] **and Dale F. Mierke*,**[†,‖]

Contribution from the Carlson School of Chemistry, Clark University, 950 Main Street, Worcester, Massachusetts 01610, Pharmaceutical Chemistry Department, School of Pharmacy, Faculty of Medicine, The Hebrew University of Jerusalem, Jerusalem 91120, Israel, Division of Bone & Mineral Metabolism, Harvard-Thorndike and Charles A. Dana Laboratories, Beth Israel Deaconess Medical Center, Harvard Medical School, 330 Brookline Avenue (HIM 944), Boston, Massachusetts 02215, and Department of Pharmacology and Molecular Toxicology, University of Massachusetts, Medical Center, 55 Lake Avenue North, Worcester, Massachusetts 01655

Received September 6, 1996[⊗]

Abstract: The conformation of a novel 1,2,5-trisubstituted hexahydro-3-oxo-1*H*-1,4-diazepine system (DAP) has been investigated by proton and carbon NMR and refined with computer simulations. Four N^1-acetyl-5-(*N,N*-dimethylamino)carbonyl DAP analogues, differing in the chirality and substituents at C2, have been studied: 2-benzyl-(2*S*,5*S*)-DAP (*SS*-**F**), 2-benzyl-(2*R*,5*S*)-DAP (*RS*-**F**), 2-methyl-(2*S*,5*S*)-DAP (*SS*-**A**), and 2-methyl-(2*R*,5*S*)-DAP (*RS*-**A**). The NMR spectra for each of the four analogues showed the presence of two configurational isomers slowly interconverting on the NMR time scale; the site of the *cis/trans* isomerization was identified as the N1-acetyl peptidic bond. The experimental restraints from NMR data consisted of a limited number of interproton distances and well-determined coupling constants; their utilization in distance geometry and distance and angle driven dynamics calculations produced high-resolution structures for three of the analogues. The C2 chirality (*R* or *S*) in the seven-membered ring determines the topological projection of the acetyl group with respect to the plane of the ring. The nature of the C2 substituent has only a small effect on the conformation of the ring and overall orientation of the N1 and C5 substituents. No significant structural differences result from the *cis* or *trans* configuration at the N1-acetyl peptidic bond. The results presented here indicate that DAP is a useful dipeptidomimetic with structural characteristics distinct from those of the widely used benzodiazepine.

Introduction

Peptidomimetics are used in drug design with the aim of constructing a non-peptide molecule which mimics the essential structural properties of a bioactive peptide and maintains some or all of the characteristic bioactivities.[1] The control of the topological arrangement of the biologically necessary residues (the pharmacophore) in peptidomimetics is accomplished by the use of molecular scaffolds.[2] The close reproduction of the bioactive molecular topology is essential in the determination of structure−activity relationships of peptidomimetic drugs and often produces molecules with improved pharmacological properties including biological activity, receptor selectivity, metabolic stability, and bioavailability.[3] The 1,4-benzodiazepines (Figure 1B), which have been successfully used in many drug systems including enkephalins,[4] cholecystokinin,[5,6] and gastrin,[6] are exemplary. In this work, we describe the confor-

mational characterization of a novel 1,2,5-trisubstituted hexahydro-3-oxo-1*H*-1,4-diazepine system (DAP) (Figure 1A) which as a peptidomimetic has distinct characteristics compared with those of the structurally similar 1,4-benzodiazepinone. As a molecular scaffold, DAP has the following characteristics: it contains two chiral centers (C2 and C5), the substituent at C2 can be predetermined through the selection of the appropriate precursor (*i* − 1) amino acid, and two positions in the heterocyclic ring (N1 and C5) can be readily modified after ring formation. Taken together, different combinations of these features could provide a molecular scaffold which can present

† Clark University.
‡ The Hebrew University.
§ Harvard Medical School.
‖ University of Massachusetts, Medical Center.
* Author to whom correspondence should be addressed: Phone: (508) 793-7220. FAX: (508) 793-8861. E-mail: dmierke@clarku.edu.
⊗ Abstract published in *Advance ACS Abstracts,* February 15, 1997.

(1) (a) Farmer P. S. In *Drug Design*; Ariens, E. J., Ed.; Academic Press: New York, 1980; Vol X, pp 119−143. (b) Giannis, A.; Kolter, T. *Angew. Chem., Int. Ed. Engl.,* **1993**, *32*, 1244−1267.

(2) Olson, G. L.; Bolin, D. R.; Pat Bonner, M.; Bos, M.; Cook, C. M.; Fry, D. C.; Graves, B. J.; Hatada, M.; Hill, D. E.; Kahn, M.; Madison, V. S.; Rusiecki, V. K.; Sarabu, R.; Sepinwall, J.; Vincent, G. P.; Voss, M. E. *J. Med. Chem.* **1993**, *36*, 3039−3049.

(3) Hruby, V. J.; Al-Obeidi, F.; Kazmierski, W. *Biochem. J.* **1990**, *268*, 249−262.

(4) Romer, D.; Buscher, H. H.; Hill, R. C.; Maurer, R.; Petcher, T. J.; Zeuger, H.; Benson, W.; Finner, E.; Milkowski, W.; Thies, P. W. *Nature (London)* **1982**, *298*, 759−760.

(5) (a) Chang, R. S. L.; Lotti, V. J.; Monaghan, R. L.; Birnbaum, J.; Stapley, E. O.; Goetz, M. A.; Albers-Schonberg, G.; Patchett, A. A.; Liesch, J. M.; Hensens, O. D.; Springer, J. P. *Science* **1985**, *230*, 177−179. (b) Evans, B. E.; Bock, M. G.; Rittle, K. E.; DiPardo, R. M.; Whitter, W. L.; Veber, D. F.; Anderson, P. S.; Freidinger, R. M. *Proc. Natl. Acad. Sci. U.S.A.* **1986**, *83*, 4918−4922. (c) Evans, B. E.; Rittle, K. E.; Bock, M. G.; DiPardo, R. M.; Freidinger, R. M.; Whitter, W. L.; Lunde II, G. F.; Veber, D. F.; Anderson, P. S.; Chang, R. S. L.; Lotti, V. J.; Cerino, D. J.; Chen, T. B.; Kling, P. J.; Kunkel, K. A.; Springer, J. P.; Hirshfield, J. *J. Med. Chem.* **1988**, *31*, 2235−2246. (d) Evans, B. E.; Rittle, K. E.; Bock, M. G.; DiPardo, R. M.; Freidinger, R. M.; Whitter, W. L.; Gould, N. P.; Lundell, G. F.; Homnick, C. F.; Veber, D. F.; Anderson, P. S.; Chang, R. S. L.; Lotti, V. J.; Cerino, D. J.; Chen, T. B.; King, P. J.; Kunkel, K. A.; Springer, J. P.; Hirshfield, J. *J. Med. Chem.* **1987**, *30*, 1229−1239. (e) Bock, M. G.; DiPardo, R. M.; Newton, R. C.; Bergman, J. M.; Veber, D. F.; Freedman, S. B.; Smith, A. J.; Chapman, K. L.; Patel, S.; Kemp, J. A.; Marshall, G. R.; Freidinger, R. M. *Bioorg. Med. Chem.* **1994**, *2*, 987−998.

(6) Bock, M. G.; DiPardo, R. M.; Evans, B. E.; Rittle, K. E.; Whitter, W. L.; Veber, D. F.; Anderson, P. S.; Freidinger, R. M. *J. Med. Chem.* **1989**, *32*, 13−16.

Diazepinone Peptidomimetic

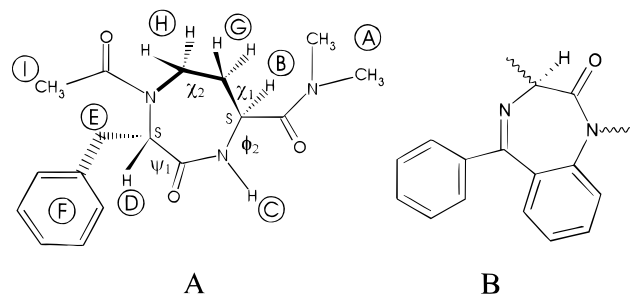*J. Am. Chem. Soc., Vol. 119, No. 10, 1997* 2431

Figure 1. Structural formula of 1,2,5-trisubstituted 1,4-diazepine-3-one (DAP) (A) and 1,4-benzodiazepine-3-one (B). The nomenclature utilized for atoms and dihedral angles in the DAP system is indicated.

a diverse range of topological arrangements of the critical pharmacophore. As a dipeptidomimetic, the DAP system presents a unique $C\alpha_i$-side-chain-to-N_{i-1}-backbone cyclization which may induce distinctive modes of local conformational constraints as compared to previously published modes of short-range molecular constraints. Unlike the structurally related 1,4-benzodiazepinone, the DAP dipeptidomimetic does not contain a fused aromatic-heterocyclic ring system which introduces a structural rigidification and increases the hydrophobicity which may contribute to limited solubility and nonspecific binding and therefore require much more elaborate substitution schemes to achieve the optimal specificity toward a designated macromolecular acceptor. In addition, the DAP, lacking the fused aromatic ring, is a more direct and general mimetic of a dipeptide unit.

In general, the conformational analysis of small peptides by NMR is beset with a number of problems not encountered in the study of other molecules of biological interest (i.e., proteins, nucleic acids). Linear peptides are naturally very flexible and can therefore quickly adopt a large number of different conformations. Secondly, the absence of secondary structural elements (i.e., α-helices, β-sheets) and high percentage of solvent exposed regions lead to small proton densities and therefore a very small number of NOEs are observed. The fact that the correlation time for the overall motion of small peptides in solution is usually not advantageous for the observation of NOEs is another element that cannot be ignored. To partially overcome these effects we have been utilizing coupling constants in the refinement of peptide conformation, in addition to the scarce number of distance constraints.[7]

Here we describe the conformational examination of four 1,2,5-trisubstituted hexahydro-3-oxo-1*H*-1,4-diazepine (DAP) analogues (*SS*-**F**/**A** and *RS*-**F**/**A**) incorporating *R* and *S* alanine and phenylalanine residues. The DAP analogues are examined in solution using proton and carbon NMR and the conformations refined with metric-matrix distance geometry and a simulated annealing protocol utilizing NOEs and coupling constants as restraints. The conformational features of DAP, which allow for more conformational variation of the projecting side chain functionalities than the structurally related 1,4-benzodiazepinone (Figure 1B), are highlighted.

Experimental Methods

Synthesis. Briefly, reductive alkylation of either *tert*-butyl (*R/S*)-phenylalaninate or *tert*-butyl (*R/S*)-alaninate with *N,N*-dimethyl (2*S*)-2-(((*tert*-butyloxy)carbonyl)amino)-4-oxobutyramide generated the linear precursor. N-Acetylation of the newly formed secondary amine was followed by acidolytic deprotection of the amino and carboxyl termini. Lactam ring formation yielded the corresponding N^1-acetyl-

5-*N′,N′*-dimethylamino)carbonyl DAP analogues, *SS*-**F**/**A** and *SR*-**F**/**A** which were purified to homogeneity on C18 reversed-phase high-performance liquid chromatography and characterized by elemental microchemical analysis, fast atom bombardment mass spectrometry, and NMR. A detailed synthesis will be published elsewhere.[8]

Nuclear Magnetic Resonance. Proton and carbon spectra were recorded on a Varian Unity 500 MHz spectrometer and processed using Varian VNMR software. The samples, approximately 30 mM, were prepared in chloroform (100% $CDCl_3$ Cambridge Isotopes). All spectra were referenced using the resonances of the solvent: 7.24 and 77.0 ppm for proton and carbon, respectively.

The proton and carbon resonance assignments were obtained in a straightforward fashion using DQF-COSY,[9] TOCSY,[10,11] NOESY,[12,13] and ROESY[14] spectra, recorded in the phase-sensitive mode using the method from States et al.[15] NOESY and ROESY spectra were collected at 250, 265, and 273 K with mixing times varying from 20 to 1000 ms; the temperature for all other experiments was 298 K. Randomization of mixing time was applied in the NOESY spectra to reduce the contribution of zero-quantum effects; in the ROESY experiments, a spin-lock field of 2500 Hz was realized by a series of short pulses as described by Kessler et al.[16] sandwiched between two 90° pulses to compensate for offset effects (compensated ROESY). The typical spectral width was 3600−4000 Hz in both dimensions, with 2048 data points in f_2 and 512 data points in f_1 and with 8−32 scans at each increment. For the assignment of carbons with directly bound protons, HMQC[17−20] spectra were recorded, with 1024 data points in the proton dimension and 10 000 Hz and 200 data points in the carbon dimension. Forward linear prediction to 1024 points and zero-filling to 2048 were applied to the incremented dimension; Gaussian apodization was used in both f_2 and f_1.

The rate of chemical exchange between the two isomers, *cis* and *trans*, was investigated by a series of one-dimensional saturation transfer experiments.[21−24] These experiments were run with temperatures varying from 288 to 313 K. The rate of exchange was obtained from a nonlinear least-squares fitting of (M/M_0) against saturation time for each temperature. The natural logarithm of the exchange rates plotted against inverse temperature provided the energy of activation, following standard procedures.

For determination of homonuclear coupling constants, the P. E. COSY[25] pulse sequence was employed. The spectra were acquired at 298 K with 4096 data points in f_2 and 640 incremental data points. The t_2 dimension was expanded with zero filling to 8196 points. HMBC[26] and HMBC with selective excitation of the carbonyl region[27,28] were recorded to obtain the magnitude of the long-range heteronuclear

(7) Eberstadt, M.; Gemmecker, G.; Mierke, D. F.; Kessler, H. *Angew. Chem., Int. Ed. Engl.* **1995**, *34*, 1671−1695.

(8) Weitz, I. S.; Pellegrini, M.; Mierke, D. F.; Chorev, M. Submitted for publication.

(9) Rance, M.; Sørensen, O. W.; Bodenhausen, G.; Wagner, G.; Ernst, R. R.; Wüthrich, K. *Biochem. Biophys. Res. Commun.* **1983**, *117*, 458−479.

(10) Braunschweiler, L.; Ernst, R. R. *J. Magn. Reson.* **1983**, *53*, 521−528.

(11) Bax, A.; Davis, D. G. *J. Magn. Reson.* **1985**, *65*, 355−360.

(12) Jeener, J.; Meier, B. H.; Bachmann, P.; Ernst, R. R. *J. Chem. Phys.* **1979**, *71*, 4546−4553.

(13) Macura, S.; Huang, Y.; Suter, D.; Ernst, R. R. *J. Magn. Reson.* **198**, *43*, 259−281.

(14) Bothner-By, A. A.; Stephens, R. L.; Lee, J.; Warren, C. D.; Jeanloz, R. W. *J. Am. Chem. Soc.* **1984**, *106*, 811−813.

(15) States, D. J.; Haberkorn, R. A.; Ruben, D. J. *J. Magn. Reson.* **1982**, *48*, 286−292.

(16) Kessler, H.; Griesinger, C.; Kerssebaum, R.; Wagner, K.; Ernst, R. R. *J. Am. Chem. Soc.* **1987**, *109*, 607−609.

(17) Muller, L. *J. Am. Chem. Soc.* **1979**, *101*, 4481−4484.

(18) Bendall, M. R.; Pegg, D. T.; Doddrell, D. M. *J. Magn. Reson.* **1983**, *52*, 81−117.

(19) Bax, A.; Griffey, R. H.; Hawkins, B. L. *J. Am. Chem. Soc.* **1983**, *105*, 7188−7190.

(20) Bax, A.; Griffey, R. H.; Hawkins, B. L. *J. Magn. Reson.* **1983**, *55*, 301−315.

(21) Forsen, S.; Hoffman, R. *J. Chem. Phys.* **1964** *40*, 1189−1196.

(22) Grathwhohl, C.; Wüthrich, K. *Biopolymers* **1981**, *20*, 2623−2633.

(23) Sanders, J. K. M.; Mersh, J. D. *Prog. NMR Specrosc.* **1982**, *15*, 353−400.

(24) Campbell, I. D.; Dobson, C. M.; Ratcliffe, R. G.; Williams, R. J. P. *J. Magn. Reson.* **1978**, *29*, 397−417.

(25) Muller, L. *J. Magn. Reson.* **1987**, *72*, 191−196.

Table 1. ^{1}H and ^{13}C Chemical Shifts (ppm, relative to TMS)

2-Methyl-(2*R*,5*S*)-DAP (*RS*-**A**)

cis (62%)

	A	B	C	D	E	G	H	I
^{1}H[a]	2.96, 2.95	4.26	6.98	4.55	1.51	2.47, 1.65	4.22, 2.95[e]	2.18
^{13}C[b]	35.8, 36.5	48.7	■	58.0	16.7	28.7	38.3	20.57[e]
^{13}C=O[c]	169.2[e]	■	170.0	■	■	■	■	170.3

trans (38%)

	a	b	c	d	e	g	h	i
^{1}H	2.99	4.44	6.79	5.21	1.37	2.15,[e] 1.80	3.80, 3.35	2.16
^{13}C	35.8, 36.5	47.9	■	55.0	15.3	30.7	41.1	20.6[e]
^{13}C=O[c]	169.0	■	170.6	■	■	■	■	169.2[e]

2-Methyl-(2*S*,5*S*)-DAP (*SS*-**A**)

cis (88%)

	A	B	C	D	E	G	H	I
^{1}H	2.99, 2.95[e]	4.42	6.55[e]	4.68	1.56	1.98[e]	4.52, 3.02	2.13
^{13}C	37.1	52.2	■	59.2	15.37	31.25	38.5	21.9
^{13}C=O[d]	170.1	■	174.0	■	■	■	■	170.9

trans (12%)

	a	b	c	d	e	g	h	i
^{1}H	2.95[e]	4.47	6.55[e]	5.24	1.51	1.98[e]	3.77, 3.58	—
^{13}C	36.4	51.0	■	55.5	—	32.7	43.3	—
^{13}C=O[d]	174.4	■	173.5	■	■	■	■	—

2-Benzyl-(2*R*,5*S*)-DAP (*RS*-**F**)

cis (73%)

	A	B	C	D	E	F	G	H	I
^{1}H[a]	2.98	4.24[e]	7.12	4.61	3.67, 2.97	e	2.55, 1.70	4.21,[e] 2.99	1.49
^{13}C[b]	35.8[e]	48.6	■	64.6	36.4	136.7,[e] 129.4[d]	28.3	38.8	19.5

trans (27%)

	a	b	c	d	e	f	g	h	i
^{1}H	2.93	4.42	6.85	5.46	3.42,[e] 3.23	e	2.03, 1.63	3.43,[e] 2.71	2.14
^{13}C	35.8[e]	48.0	■	60.2	34.4	137.1,[e] 130.0[d]	30.2	42.8	20.8

2-Benzyl-(2*S*,5*S*)-DAP (*SS*-**F**)

cis (86%)

	A	B	C	D	E	F	G	H	I
^{1}H	3.00, 2.94	4.43	6.63	4.79	3.46, 3.12[e]	e	2.24, 2.08	4.40, 3.04[e]	1.65
^{13}C	36.4, 36.8	52.4	■	65.4	35.6	136.6	30.0	38.6	20.6

trans (14%)

	a	b	c	d	e	f	g	h	i
^{1}H	—	—	6.79	5.55	—	e	—	—	—
^{13}C	36.4, 36.8	—	■	—	—	—	—	—	—

^{a} From 1D proton spectrum and TOCSY spectrum (— minor resonance not assigned). ^{b} From ^{1}H−^{13}C HMQC spectrum. ^{c} From ^{1}H−^{13}C selective HMBC spectrum. ^{d} From ^{1}H−^{13}C HMBC spectrum. ^{e} Overlapping resonances.

coupling constants, $^3J_{\text{C−H}}$. Spectral widths of 25 000 and 2000 Hz for the carbon dimension were used for the HMBC and selective HMBC, respectively, with 512 data points acquired in both cases.

Distance Geometry. The distance geometry (DG) calculations were carried out with a home-written program utilizing the random metrization algorithm of Havel.[29] Experimentally determined distances (calculated using the isolated two-spin approximation) were adjusted by ±10% to produce upper and lower distance restraints. This range has been shown to be sufficient for errors in integration and differing correlation times. The error range also accounts for the variation in cross-peak intensities from chemical exchange.[30,31] Only NOEs which produce distance restraints more restrictive than the geometric distance bounds (holonomic restraints)[32] are subsequently utilized to create the final distance matrix. Distances between the upper and lower bounds, which also satisfy the triangular inequality law, were then chosen randomly using the random metrization procedure.[29]

The structures were first embedded in four dimensions and then partially minimized using conjugate gradients followed by distance and angle driven dynamics (DADD);[33−35] the DADD simulation was carried

(26) Bax, A.; Summers, M. F. *J. Am. Chem. Soc.* **1986**, *108*, 2093−2094.

(27) Bermel, W.; Wagner, K.; Griesinger, C. *J. Magn. Reson.* **1987**, *83*, 223−232.

(28) Kessler, H.; Schmieder, P.; Köck, M.; Kurz, M. *J. Magn. Reson.* **1990,** *88*, 615−618.

(29) Havel, T. F. *Prog. Biophys. Mol. Biol.* **1991**, *56*, 43−78

(30) Choe, B.; Cook, G. W.; Krishna, N. R. *J. Magn. Reson.* **1991,** *94*, 387−393.

(31) Lee, W.; Krishna, N. R. *J. Magn. Reson.* **1992,** *98*, 36−48.

(32) Crippen, G. M.; Havel, T. F. *Distance Geometry and Molecular Conformation*; Research Studies Press LTD: Somerset, England; John Wiley, New York, 1988.

Table 2. Rates of Exchange between *cis* and *trans* Configurational Isomers in CDCl$_3$ at 25 °C

molecule	%*cis*	rate (s^{-1})		$\Delta G^{\ddagger}$ (kJ mol^{-1})		E_a (kJ mol^{-1})	
		$c \rightarrow t$	$t \rightarrow c$	$c \rightarrow t$	$t \rightarrow c$	$c \rightarrow t$	$t \rightarrow c$
SS-**F**	86	2.42	14.3	70.8	66.4	50.9	48.6
RS-**F**[a]	73	—	1.4	—	72.1	—	—
SS-**A**	88	3.13	13.6	70.2	66.5	57.4[b]	65.5[b]
RS-**A**	62	0.95	0.98	74.3	73.0	42.5	36.6

[a] The $c \rightarrow t$ rate was too slow to measure. Accurate measurement of the energy barrier could not be obtained since lowering of the temperature reduced the exchange rate and the solvent limited the increase of the temperature. [b] The error associated with these values are particularly high, caused by the very small population of the *trans* configurational isomer and therefore the very low signal-to-noise ratio when integrating the peaks during the saturation transfer experiments. Of course, the activation energy for $t \rightarrow c$ should be smaller than for the $c \rightarrow t$.

out at 1000 K for 50 ps and then there was a gradual reduction in temperature over the next 30 ps. The DADD procedure utilizes the holonomic and experimental distance constraints plus a chiral penalty function for the generation of the violation "energy" and forces. A distance matrix was calculated from each structure and the EMBED algorithm[32] used to calculate coordinates in 3D. The optimization and DADD procedure were then repeated.

The following ensemble calculations[36–38] are identical to those used for the DADD method, except that the penalty expression for the experimental restraints (NOEs and coupling constants)[7,38–40] and the forces calculated from these restraints are generated from an ensemble average. The metrization and refinement of 100 structures required approximately 2 h of cpu using a single processor on a SGI Indigo2 (R4400). Energy minimizations and interactive modeling were performed using *Discover* (Consistent Valence Force Field) and Insight II (Biosym Technologies Inc., San Diego, CA).

Results

The one-dimensional ^{1}H-NMR spectra indicate two complete sets of signals for each peptide. The ^{1}H and ^{13}C resonance assignments from TOCSY, DQF-COSY, HMQC, and HMBC spectra are given in Table 1. Exemplary NMR spectra for *SS*-**A** and *RS*-**A** are given in the Supporting Information. Exchange between the two signal sets was evident in ROESY and NOESY spectra. The major conformer contains a *cis* configuration about the N1-acetyl peptidic bond, as determined by the presence of NOEs between the acetyl CH$_3$ and the methyl or benzyl group on C2 in the alanine- and phenylalanine-containing analogues, respectively. A large difference in the ^{1}H and ^{13}C chemical shifts of the atoms adjacent to the acetyl bond is observed between the two configurational isomers (*cis* and *trans*), consistent with this assignment. In addition, NOEs implying a *trans* configuration were observed for the minor isomers. The rate of chemical exchange is greatly affected by the relative chirality of C2 (belonging to the phenylalanyl and alanyl residues) and C5. The results of the analysis of the chemical exchange as a function of temperature are given in Table 2. The ratio of the two configurations is only slightly affected by

(33) Kaptein, R.; Boelens, R.; Scheek, R. M.; van Gunsteren, W. F. *Biochemistry* **1988**, *27*, 5389–5395.
(34) Mierke, D. F.; Kessler, H. *Biopolymers* **1993**, *33*, 1003–1017.
(35) Mierke, D. F.; Geyer, A.; Kessler, H. *Int. J. Pept. Protein Res.* **1994**, *44*, 325–331.
(36) Scheek, R. M.; van Gunsteren, W. F.; Kaptein, R. *Methods in Enzymology*; Oppenheimer, N. J., James, T. L., Eds.; Academic Press: New York, 1989; Vol. 177, pp 204–218.
(37) van Nuland, N. A. J.; Grötzinger, J.; Dijkstra, K.; Scheek, R. M.; Robillard, G. T. *Eur. J. Biochem.* **1992**, *210*, 881–891.
(38) Mierke, D. F.; Kurz, M.; Kessler, H. *J. Am. Chem. Soc.* **1994**, *116*, 1042–1049.
(39) Mierke, D. F.; Kessler, H. *Biopolymers* **1992**, *32*, 1277–1282.
(40) Mierke, D. F.; Scheek, R. M.; Kessler, H. *Biopolymers* **1994**, *34*, 559–563.

Table 3. Experimental Distances (Upper Limits) Derived from NOESY and ROESY Spectra, As Utilized in the Distance Geometry Calculations (subscripts 1 and 2 indicate prochiralities *pro-R* and *pro-S*, respectively)

proton	proton	distance (Å)
	RS-**F** (cis)	
F	I	5.0
B	A	5.0
C	G$_1$	3.7
C	B	3.0
D	I	4.4
	RS-**F** (trans)	
C	A	4.0
H$_1$	I	4.0
	SS-**F** (cis)	
B	A	4.5
C	B	4.3
E$_2$	I	3.2
D	I	4.0
	RS-**A** (cis)	
B	A	4.1
B	D	4.0
C	G$_1$	4.5
H$_2$	E	3.5
	RS-**A** (trans)	
B	A	4.1
B	D	3.2
C	G$_1$	4.5
H$_2$	E	3.5
H$_2$	D (α-carbon)	3.0[a]
H$_1$	D (α-carbon)	> 3.3[a]

[a] Distances calculated from analysis of heteronuclear coupling constants.

temperature, for example, *RS*-**F**, 2.7 *cis/trans* at 298 K and 2.8 at 288 K; *SS*-**F**, 6.2 *cis/trans* at 298 K and 7.2 at 213 K; *RS*-**A**, 1.6 *cis/trans* at 298 K; *SS*-**A**, 7.6 *cis/trans* at 298 K.

The generation of distance restraints from the ROESY and NOESY spectra was problematic. The fast chemical exchange between the configurational isomers placed severe restrictions on the mixing times. Spectra acquired with mixing times of 200 ms were dominated by chemical exchange. Attempts to slow down the rate of exchange with a decrease in temperature (250 K) did not significantly improve the spectra. Therefore, the number of conformationally informative experimental distances is limited (listed in Table 3). This is not surprising given the small number of protons of the peptides. Hence, emphasis was placed on the conformational information contained in vicinal coupling constants.[7,38,39]

Concerning the *SS*-**A** analogue, the severe overlap of signals, both within and between each configurational isomer, along with an extremely fast chemical exchange, prohibited the acquisition of any structurally relevant data from NOESY or P. E. COSY spectra. Therefore, the conformation of this analogue will not be further discussed. In addition, the small concentration (approximately 13%) prohibited further analysis of the *trans* isomer (minor configurational isomer) of *SS*-**F**.

The ^3J proton–proton coupling constants obtained from P. E. COSY spectra are reported in Table 4. These couplings along with the long-range heteronuclear couplings from the HMBC allowed for the diastereotopic assignment of the methylene protons of the ring system (corresponding to C6 and C7) and the benzyl group on C2 (Phe side chain). These assignments were confirmed by the NOEs noted in Table 3. An expanded portion of a P. E. COSY spectrum illustrating the extraction of multiple coupling constants from one cross peak is given in Figure 2. These coupling constants were used directly as experimental restraints in DG calculations, following procedures developed in our laboratory.[7,38–40]
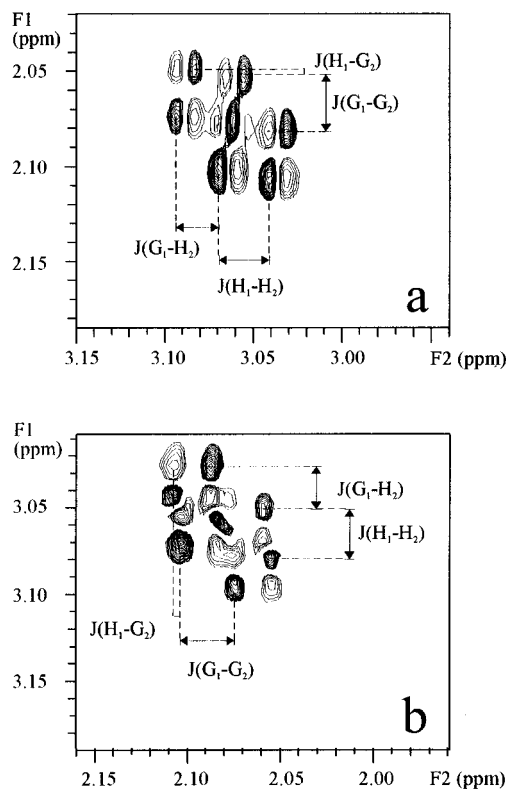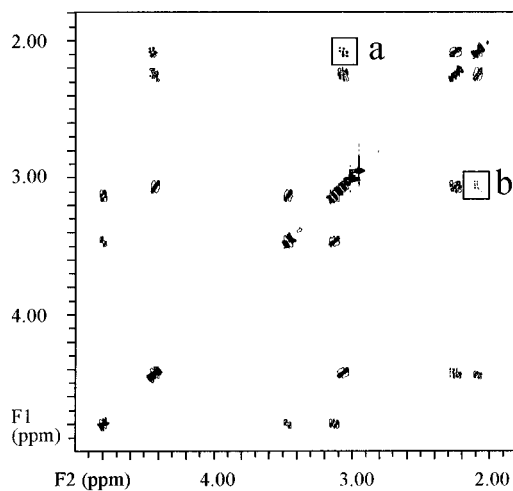
Figure 2. Expanded portion of a P. E. COSY spectrum of *SS*-**F** DAP in CDCl$_3$ at 298 K. The extraction of $^2J_{HH}$ and $^3J_{HH}$ coupling constants from the cross-peak fine structure is illustrated.

Table 4. ^3J Proton−Proton Coupling Constants (Hz) Obtained from P. E. COSY Spectra (subscripts 1 and 2 indicate prochiralities *pro-R* and *pro-S*, respectively)

		RS-**F** (*cis*)	
$J(D-E_1)$	3.4	$J(G_1-H_1)$	7.6
$J(D-E_2)$	10.5	$J(G_1-H_2)$	1.9
$J(B-C)$	5.0	$J(G_2-H_1)$	9.5
$J(B-G_1)$	11.4	$J(G_2-H_2)$	9.5
$J(B-G_2)$	3.8		
		RS-**F** (*trans*)	
$J(D-E_1)$	6.7	$J(G_1-H_1)$	1.9
$J(D-E_2)$	2.9	$J(G_1-H_2)$	6.6
$J(B-C)$	5.7	$J(G_2-H_1)$	7.6
$J(B-G_1)$	11.9	$J(G_2-H_2)$	11.4
$J(B-G_2)$	3.9		
		SS-**F** (*cis*)	
$J(D-E_1)$	10.2	$J(G_1-H_1)$	12.1
$J(D-E_2)$	3.7	$J(G_1-H_2)$	5.6
$J(B-C)$	7.9	$J(G_2-H_1)$	3.7
$J(B-G_1)$	5.7	$J(G_2-H_2)$	2.7
$J(B-G_2)$	5.6		
		RS-**A** (*cis*)	
$J(B-C)$	6.8	$J(G_1-H_2)$	6.8
$J(B-G_1)$	12.7	$J(G_2-H_1)$	7.8
$J(B-G_2)$	3.9	$J(G_2-H_2)$	9.8
$J(G_1-H_1)$	1.9		
		RS-**A** (*trans*)	
$J(B-C)$	6.8	$J(G_1-H_2)$	6.8
$J(B-G_1)$	11.7	$J(G_2-H_1)$	7.8
$J(B-G_2)$	3.9	$J(G_2-H_2)$	11.2
$J(G_1-H_1)$	1.0		

The random metrization and DADD simulations utilizing both NOE and coupling constant restraints produced 90−95 conformations with small violation energies. Each of the structures was copied five times to create a starting point for the ensemble calculations. Two additional simulations using (1) only NOEs and (2) *no* experimental restraints were carried out to examine the effect of the different experimental constraints (NOE and

coupling constants) and the intrinsic conformational "constraint" of the ring (i.e., the constraint introduced from cyclization). The results from the calculation of *RS*-**A** (*cis*) analogue (major configurational isomer) are shown in the form of Ramachandran plots in Figure 3 for the three sets of calculations. The values of the dihedral angles for the major isomers (*cis*) of *RS*-**A**, *RS*-**F**, and *SS*-**F** are reported in Table 5.

In Figure 4, the results from the *free* simulations (no experimental restraints) are shown. The restriction in the conformational freedom of the ring system introduced by the benzyl ring of the phenylalanine (compared to the methyl group of the alanine residue) is clearly illustrated.

Discussion

The 1,2,5-trisubstituted 1,4-diazepinone (DAP) structure is derived from an ethylene-mediated cyclization between the main chain N$_{i-1}$ amide nitrogen and the side chain of the subsequent (*i*) amino acid, generating a seven-membered lactam ring. N1 acetylation yields an exocyclic tertiary amide which resembles that found in the naturally occurring N-acylated proline. In this regard DAP is a true dipeptidomimetic which, as with the closely related 1,4-benzodiazepine-3-one, can be incorporated in different peptide sequences to control the spatial orientation of the preceding (*i* − 2) and following (*i* + 1) residues.

The aim of this research is to develop molecular tools which will help obtain peptide drugs that afford the conformational requirements for biological activity. In addition, the introduction of the peptidomimetic increases the stability against enzymatic degradation and allows for alteration of the physical properties that may increase the crossing of the blood-brain-barrier, an important feature for CNS active peptide-based drugs. Here the conformational characteristics of novel dipeptide-derived DAPs have been investigated using NMR and DG calculations.

The investigation of the *cis/trans* isomerization finds high rate constants, ranging from 1 to 15 s^{-1} (Table 2), where
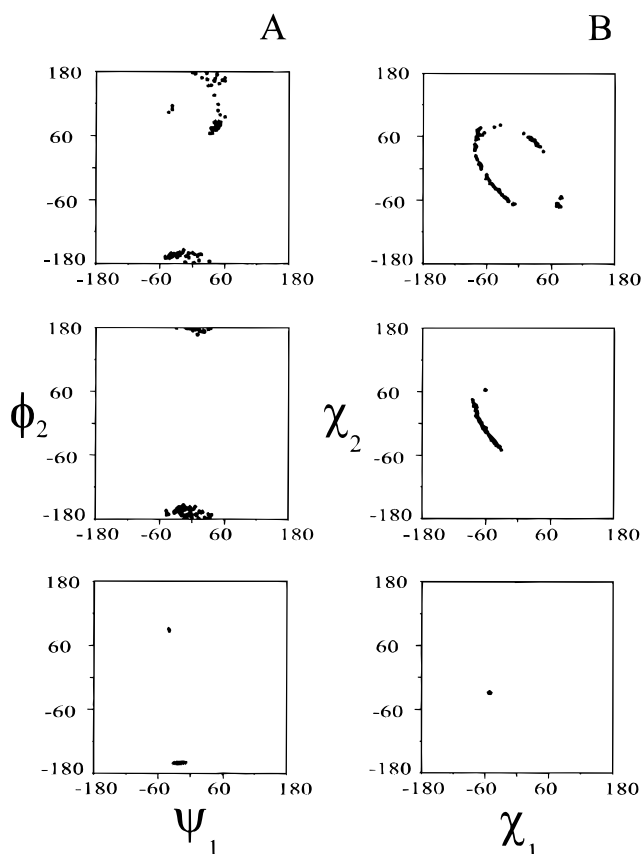
Figure 3. Ramachandran maps illustrating the application of the experimental restraints for *RS*-**A**: (top) no experimental restraints, (middle) only NOEs, (bottom) both coupling constants and NOEs. Panel A: ψ_1 and ϕ_2, Panel B: χ_1 and χ_2.

Table 5. Values for the Dihedral Angles (deg) in the Seven-Membered Ring of the Major Isomers of *RS*-**A**, *RS*-**F**, and *SS*-**F** Obtained after Energy Minimization of the DG Structures (the nomenclature used for the dihedral angles is indicated in Figure 1)

	RS-**A** (*cis*)	*RS*-**F** (*cis*)	*SS*-**F** (*cis*)
ϕ_1	139	128	−110
ψ_1	−20	43	−51
ϕ_2	−164	161	−171
χ_1	−49	−71	−77
χ_2	−31	63	68
χ_3	79	5	−67

standard values for *cis/trans* isomerization at the X-Pro peptide bond are lower than 10^{-2} s^{-1}.[22] Higher rates are observed for the *SS*-**F/A** compounds compared to the *RS*-**F/A**. The thermodynamic parameters are slightly smaller than those measured for isomerization about prolines.[22] This is not overly surprising given that, although both of these systems contain a tertiary amide at the site of isomerization, the ring system of proline is markedly smaller. The $\Delta G^{\ddagger}$ values calculated for the *RS*-**F/A** DAP analogues are slightly larger than for the corresponding *SS*-**F/A** analogues; these chirality-related differences find, of course, no correspondence in the X-Pro systems.

Interesting results have been obtained in the determination of the conformational freedom of the DAP analogues or equivalently the intrinsic conformational constraint induced by the small ring size. As illustrated in Figure 4 for the dihedral angles about the −C6−C7− ethylene linker (χ_1 and χ_2), each of the three examined analogues can access only a limited part of the conformational space. The 2000 structures calculated with *no* restraints occupy a "ring"-shaped conformational space on the Ramachandran map for both of the *RS*-**F/A** analogues, while the *SS*-**F** analogue can occupy only two small regions of
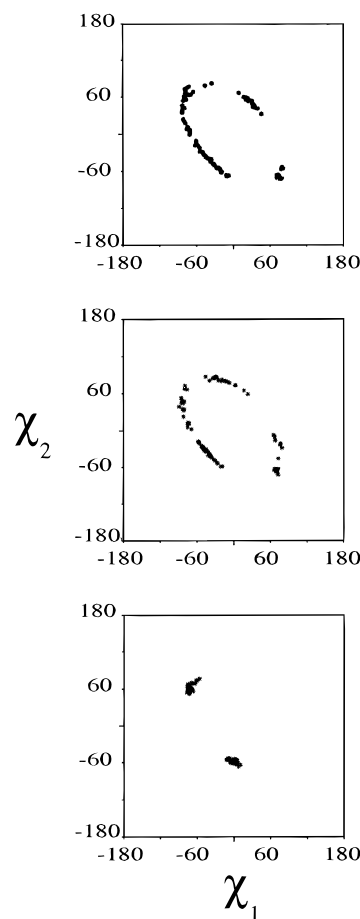

Figure 4. Ramachandran maps for the dihedral angles χ_1 and χ_2 resulting from the *free* simulation of 2000 structures: *RS*-**A** (top), *RS*-**F** (middle), *SS*-**F** (bottom). The effects of cyclization and chirality on the accessible conformational space is clearly demonstrated.

this "ring." This illustrates not only the utility of the short-range cyclization for the introduction of conformational constraint but also the relevance of the chirality of the ($i − 1$) amino acid, incorporated in the DAP system, in controlling the extent and the nature of the conformational constraint.

In addition to the general conformational characterization of the DAP system as a novel dipetidomimetic, the conformations of the four DAP analogues studied here allow us to address two other questions related to the nature of the ($i − 1$) amino acid residue: (1) the effect of the substituent on C2, namely, methyl vs benzyl (alanine vs phenylalanine) and (2) the role of the chirality of C2 on the conformation of the DAP ring system. To answer the former question, the conformations of the *RS*-**A** and *RS*-**F** DAP analogues are compared, while a comparison of the *SS*- and *RS*-**F** DAP analogues will address the latter. The problems encountered with the conformational analysis of the *SS*-**A** DAP analogue, as noted above, excluded this analogue from further consideration.

The chirality at the C2 has a significant effect on the conformation of the DAP ring system. To reduce steric interactions the benzyl side chain must adopt an axial (pseudo-axial) position. This produces an up−down ("zigzag") effect on the following nitrogen of the tertiary amide, N1 (Figure 5). The conformational consequences are pronounced: the acetyl group (which represents a potential N-terminal portion of a DAP-incorporated peptide) is projecting in different directions; the *SS*-**F** DAP analogue has the acetyl group above the "average" plane of the seven-membered ring, while the *RS*-**F** DAP analogue has the acetyl group below that plane (see Figure
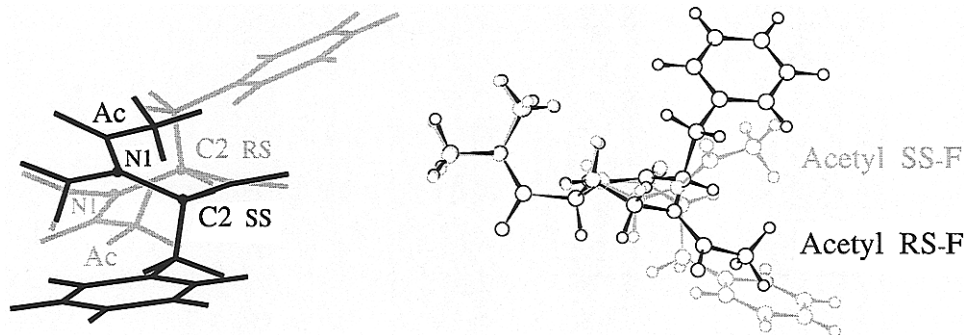
Figure 5. Superposition of the structures of *RS*-**F** (in black) and *SS*-**F** (in gray) illustrating the "zigzag" effect induced by the opposite chirality to reduce steric interaction: The side chain, benzyl, must adopt an axial (pseudo-axial) position. The structures have been energy minimized. Left panel: Only a portion of the ring is shown for clarity. The view is from the acetyl-group side of the ring and the structures are superimposed utilizing the remaining atoms of the ring. Right panel: The N1-acetyl group is projecting in different directions; the *SS* (gray) has the N1-acetyl group above the plane of the seven-membered ring, and the *RS* (black) has the N1-acetyl group below the plane.
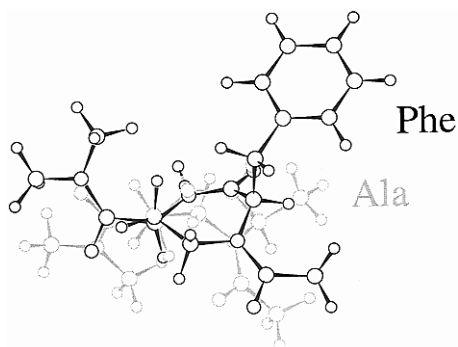
Figure 6. Superposition of the *RS*-**F** and *RS*-**A**: the C2-benzyl side chain adopts an axial orientation more pronounced than the C2-methyl. Note that the atoms of the ring system can be superimposed almost perfectly, except for the shift in the orientation of the C7-methylene group. The structures have been energy minimized.

5). In both diastereomers the N1-acetyl and the C2-benzyl project in opposite directions.

The type of substituent at the C2 position has a much more subtle effect on the conformation of the DAP ring than the C2 chirality discussed above; the change from C2-methyl (as in the *i* − 1 alanyl residue) to C2-benzyl (as in the *i* − 1 phenylalanyl residue) has almost no impact on the positioning of the N1-acetyl group. The benzyl moiety, as in *RS*-**F** DAP, prefers a more pronounced axial orientation than that found for the C2-methyl-containing *RS*-**A** DAP analogue. This difference forces a change in the orientation of the C7-methylene group of the seven-membered ring, which is necessary to relieve some of the steric hindrance between the C2-benzyl side chain and the C7-methylene group. All of the other atoms in the DAP ring system of the two diastereomers *RS*-**A** and *RS*-**F** are unaffected and remain almost perfectly superimposable (Figure 6).

The close similarity in the spatial orientation of the N1-acetyl group in *RS*-**A** and *RS*-**F** DAP analogues is important in the utilization of the DAP system in drug design. It strongly suggests indifference of the overall topological arrangements regardless of the *i* − 2 and *i* + 1 amino acids substituting N1 and the carboxyl on C5 of the DAP ring. There are indeed limited local conformational effects, but no significant global consequences are observed. Eventually, this conformational characteristic will be further examined by incorporating the DAP-based dipeptidomimetic into longer peptide sequences.

A comparison of the *RS*-**A** and *SS*-**F** DAP analogues reveals a more complicated conformational relation (Figure 7) than those described above: *RS*-**A** vs *RS*-**F** and *RS*-**F** vs *SS*-**F**. The differing chiralities of the amino acids within the ring system
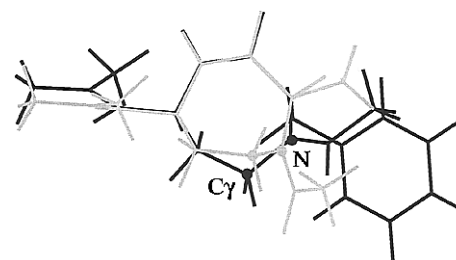

Figure 7. Superposition of the *RS*-**A** (in gray) and *SS*-**F** (in black) illustrating the similarity in ring conformation; only the −C7−N1− unit cannot be superimposed. The structures have been energy minimized.

lead to very different projections of the N1-acetyl, while the axial positioning of the C2-benzyl substituent forces a displacement of the C7-methylene to minimize the steric 1,3-interactions. The combination of both of these effects results in DAP ring conformations that are quite similar; only two of the ring atoms, −C7−N1−, cannot be superimposed.

Conclusions

Four 1,2,5-trisubstituted 1,4-diazepine-3-one dipeptidomimetics containing a *cis* intracyclic peptide bond and incorporating *R/S*-**A**la or *R/S*-Phe have been conformationally examined using NMR and computer simulations. The differences in conformation induced by the variation of chirality and of the C2 side chain have been fully characterized, thus comprise the first step in the possible utilization of DAP as a dipeptidomimetic. Our findings indicate that DAP affords control of the topological orientation of the amino acids extending from the seven-membered ring system. This conformational control realized without fusing the seven-membered heterocyclic ring with a benzene should make the DAP-based dipeptidomimetic an attractive alternative to the commonly used 1,4-benzodiazepines.

Supporting Information Available: The 2D-NMR TOCSY and HMQC spectra for the *RS*-**A** and *SS*-**A** analogues (4 pages). See any current masthead page for ordering and Internet access instructions.

JA963144F